

Eastern North Pacific Hurricane Season of 1997

MILES B. LAWRENCE

Tropical Prediction Center, National Weather Service, National Oceanic and Atmospheric Administration, Miami, Florida

(Manuscript received 15 June 1998, in final form 20 October 1998)

ABSTRACT

The hurricane season of the eastern North Pacific basin is summarized and individual tropical cyclones are described. The number of tropical cyclones was near normal. Hurricane Pauline's rainfall flooding killed more than 200 people in the Acapulco, Mexico, area. Linda became the strongest hurricane on record in this basin with 160-kt 1-min winds.

1. Introduction

Tropical cyclone activity was near normal in the eastern North Pacific basin (east of 140°W). Seventeen tropical cyclones reached at least tropical storm strength (≥ 34 kt) ($1 \text{ kt} = 1 \text{ n mi h}^{-1} = 1852/3600$ or $0.514 444 \text{ m s}^{-1}$) and nine of these reached hurricane force (≥ 64 kt). The long-term (1966–96) averages are 15.7 tropical storms and 8.7 hurricanes. Table 1 lists the names, dates, maximum 1-min surface wind speed, minimum central pressure, and deaths, if any, of the 1997 tropical storms and hurricanes, and Figs. 1a–c show their tracks.

Seven hurricanes attained 1-min sustained surface wind speeds of 100 kt or greater (category three on the Saffir–Simpson hurricane scale) and Hurricane Linda reached an unprecedented 160 kt. For comparison, the long-term average number of 100-kt or greater hurricanes is 3.7 and there have been as many as eight such hurricanes during a season.

Although the El Niño is not well defined (Trenberth 1997), the El Niño of 1997–98 was an area of anomalously warm sea surface temperatures (SST) centered along the equator and extending from the South American coast westward to near the international date line. Peak anomalies in 1997 reached +5°C near 100°W and this El Niño is, perhaps, the strongest on record.

The El Niño area of positive SST anomalies was located just south of the 1997 tropical cyclone tracks and, during most of the season, SSTs near the tracks were generally from 0° to +1°C above normal. There was a small area of +3°C anomaly along the coast of Baja California that was not part of the El Niño anomaly, but only two tropical cyclones were near this second

anomaly. Whitney and Hobgood (1997) show by stratification that there is little difference in the frequency of eastern Pacific tropical cyclones during El Niño years and during non-El Niño years. However, they did find a relation between SSTs near tropical cyclones and the maximum intensity attained by tropical cyclones. This suggests that the slightly above-normal SSTs near this year's tracks contributed to the seven hurricanes reaching 100 kt or more.

In addition to the infrequent conventional surface, upper-air, and radar observations, most of the data used to determine the tropical cyclone tracks and intensity during 1997 were derived from satellites. There were also a few reconnaissance missions into Hurricanes Guillermo and Linda.

In the individual storm summaries in section 2, it is indicated when data other than satellite data were available to determine track and intensity. The individual summaries often contain descriptions of the large-scale wind patterns affecting a storm. This information comes from whatever wind observations were available, including satellite cloud-motion wind vectors and wind analyses from global numerical models.

Section 3 gives a brief summary of the verification errors of the official National Hurricane Center (NHC, now known as the Tropical Prediction Center) forecasts for the 1997 eastern Pacific season.

2. Individual tropical storms and hurricanes

a. Tropical Storm Andres, 1–7 June

Tropical Storm Andres moved toward the east to southeast, near the coast of Central America, for several days. This eastward-moving track, in this location, with the associated weather that affected Central America, is unprecedented in the more than 700 eastern Pacific tropical cyclone tracks of record since 1949.

Corresponding author's address: Miles Lawrence, Tropical Prediction Center, 11691 S.W. 17 St., Miami, FL 33165-2149.
E-mail: lawrence@nhc.noaa.gov

TABLE 1. Eastern North Pacific basin tropical storms and hurricanes, 1997.

Number	Name	Class*	Dates**	Max. 1-min. wind speed (k)	Min. sea level Press. (mb)	Deaths
1	Andres	T	0–7 Jun	45	998	
2	Blanca	T	9–12 Jun	40	1002	
3	Carlos	T	25–28 Jun	45	996	
4	Dolores	H	5–12 Jul	80	975	
5	Enrique	H	12–16 Jul	100	960	
6	Felicia	H	14–22 Jul	115	948	
7	Guillermo	H	30 Jul–15 Aug	140	919	
8	Hilda	T	9–15 Aug	45	1000	
9	Ignacio	T	17–19 Aug	35	1005	
10	Jimena	H	25–30 Aug	115	942	
11	Kevin	T	3–7 Sep	50	994	
12	Linda	H	9–17 Sep	160	902	
13	Marty	T	12–16 Sep	40	1002	
14	Nora	H	16–26 Sep	115	950	2 (Mexico)
15	Olaf	T	26 Sep–12 Oct	60	989	
16	Pauline	H	5–10 Oct	115	948	230 + (Mexico)
17	Rick	H	7–10 Nov	75	980	

* T: tropical storm, wind speed 34–63 k. H: hurricane, wind speed 64 k or higher.

** Dates begin at 0000 UTC and include tropical depression stage.

The upper-level westerlies extended to rather low latitudes over the eastern North Pacific Ocean through most of the month of May. The associated westerly vertical wind shear helped inhibit tropical cyclone formation in that basin during May. Near the end of the month, however, the westerlies lifted northward slightly over the easternmost part of the basin. It was there that a distinct circulation of low- to midlevel clouds developed on 30 May, possibly in association with a tropical wave that crossed the Atlantic Ocean at low latitudes from 14 to 28 May. On 31 May, deep convection developed and became concentrated near the center of the cloud pattern. The disturbance became a tropical depression at 0000 UTC on 1 June, about 300 n mi (1 n mi = 1852 m) south of the Gulf of Tehuantepec.

As the cloud pattern became elongated generally from north to south on 2–3 June, a second cloud center to the north-northwest of the original center became dominant. The cyclone strengthened slightly early in this period and became Tropical Storm Andres.

Andres initially moved toward the northwest. This track gradually brought the tropical storm into a pattern of westerly steering winds and, by midday of 3 June, the storm was moving toward the east to east-northeast. This heading was toward land and the first in a series of tropical storm watches and warnings for southeastern Mexico and Central America was issued. Andres moved to within about 30 n mi of the coast of Guatemala and strengthened a little, to its maximum intensity of 45 kt.

The axis of a short-wave trough passed a little to the north, over the Bay of Campeche, on 4 June. The northwesterly flow behind the axis steered Andres toward the southeast on a course roughly parallel to the coast. On this track, Andres' cloud pattern became rather shapeless while the cyclone interacted increasingly with in-

tertropical convergence zone (ITCZ) clouds and a monsoonlike circulation associated with the ITCZ. The storm then weakened.

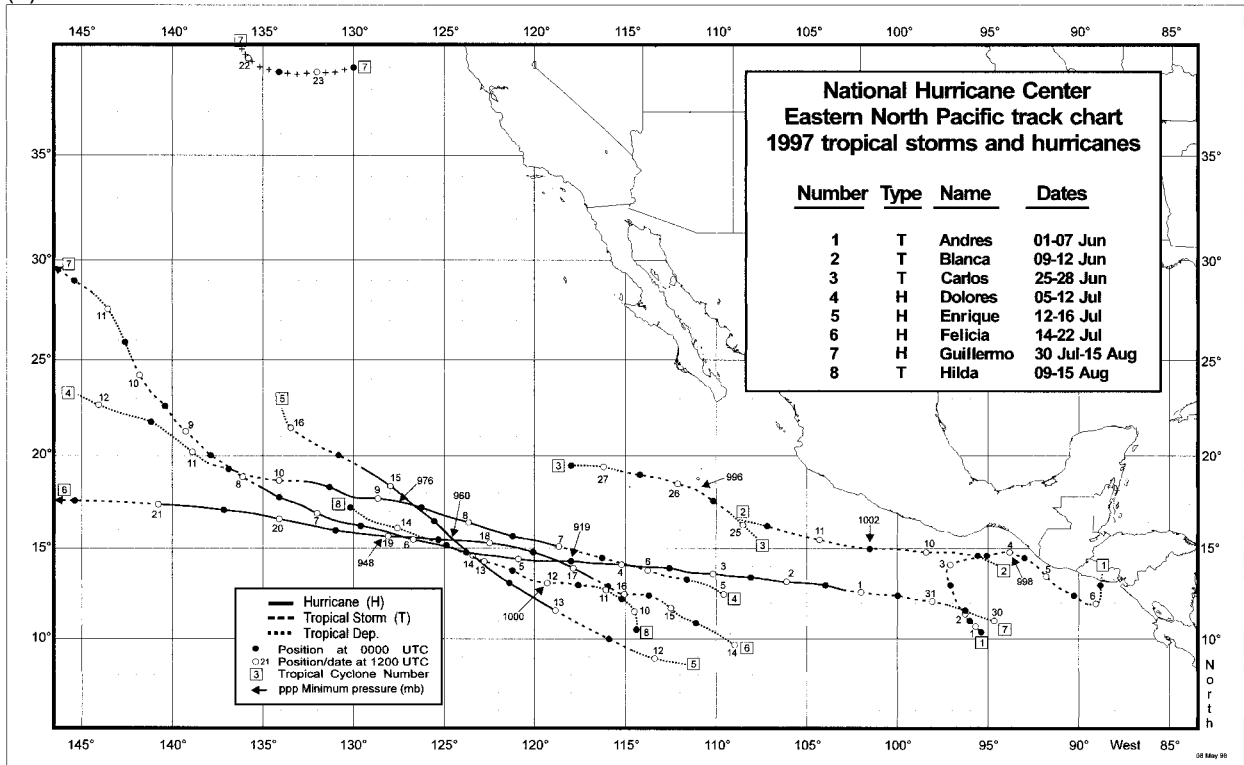
Late on 6 June, Andres began moving northward and made landfall on the coast of El Salvador near 0000 UTC on 7 June as a tropical depression. It was the first tropical cyclone landfall in that country since track records began in 1949.

The surface circulation became disrupted by the high terrain of Central America and is estimated to have dissipated a few hours after landfall. A midlevel cloud remnant continued to circulate and move northward over land. When that feature reached the Gulf of Honduras, a weak surface low redeveloped. Eventually, the rejuvenated system contributed to heavy rain over western Cuba, the southern Florida peninsula, and the northwestern Bahamas. The low gradually combined with a weak, nontropical trough over the eastern Gulf of Mexico.

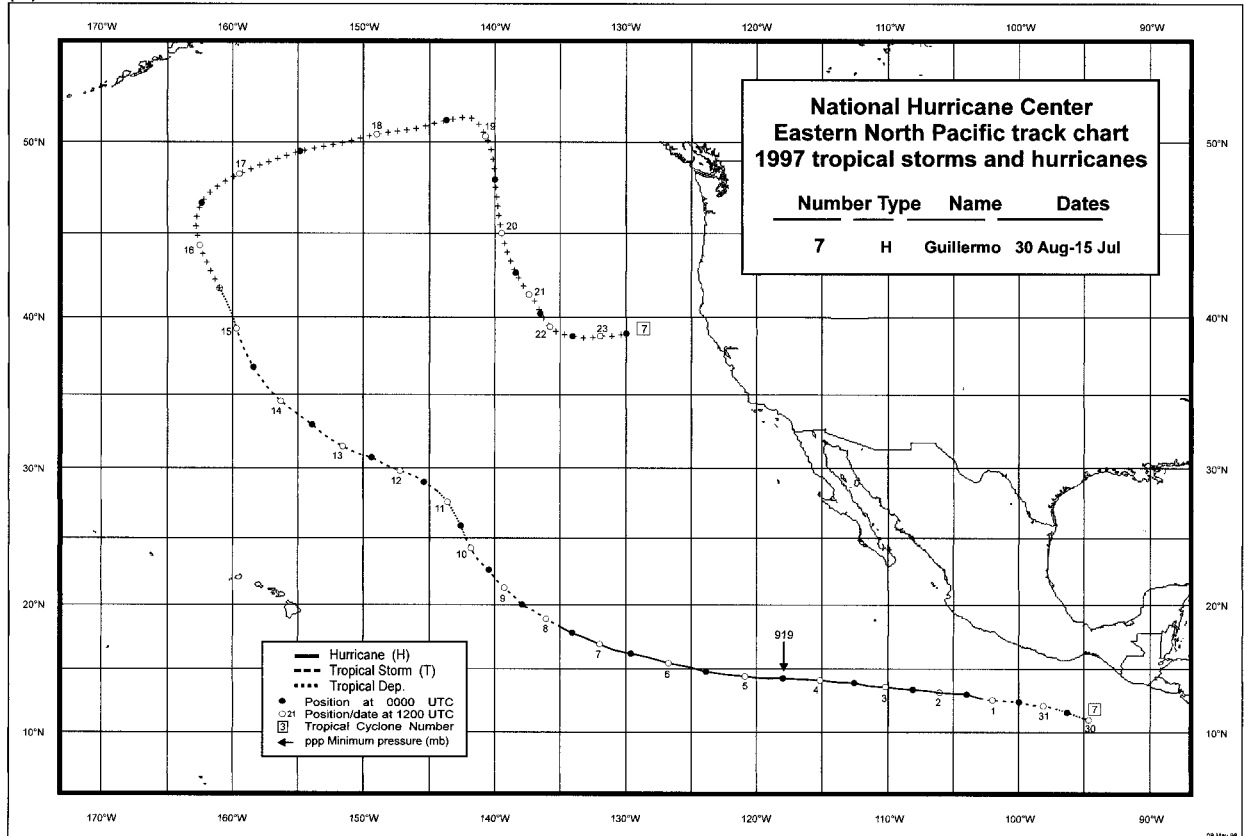
The operational analyses of Andres' surface wind field were enhanced by wind speed and direction data received from a National Aeronautics and Space Administration scatterometer. However, these data were available only briefly before satellite technical difficulties occurred.

According to *El Nuevo Herald*, Andres generated torrential showers and locally enormous seas and inundations along the western Central America coast. A reprinting of Nicaragua's *La Prensa* by *El Nuevo Herald* indicated that two fishermen were missing. There were no other reports of casualties. *El Nuevo Herald* attributed to Andres interruptions to electricity, overflowing rivers, automobile accidents, and damage to about 10 homes in El Salvador and Nicaragua. Damage was noted

(a)



(b)



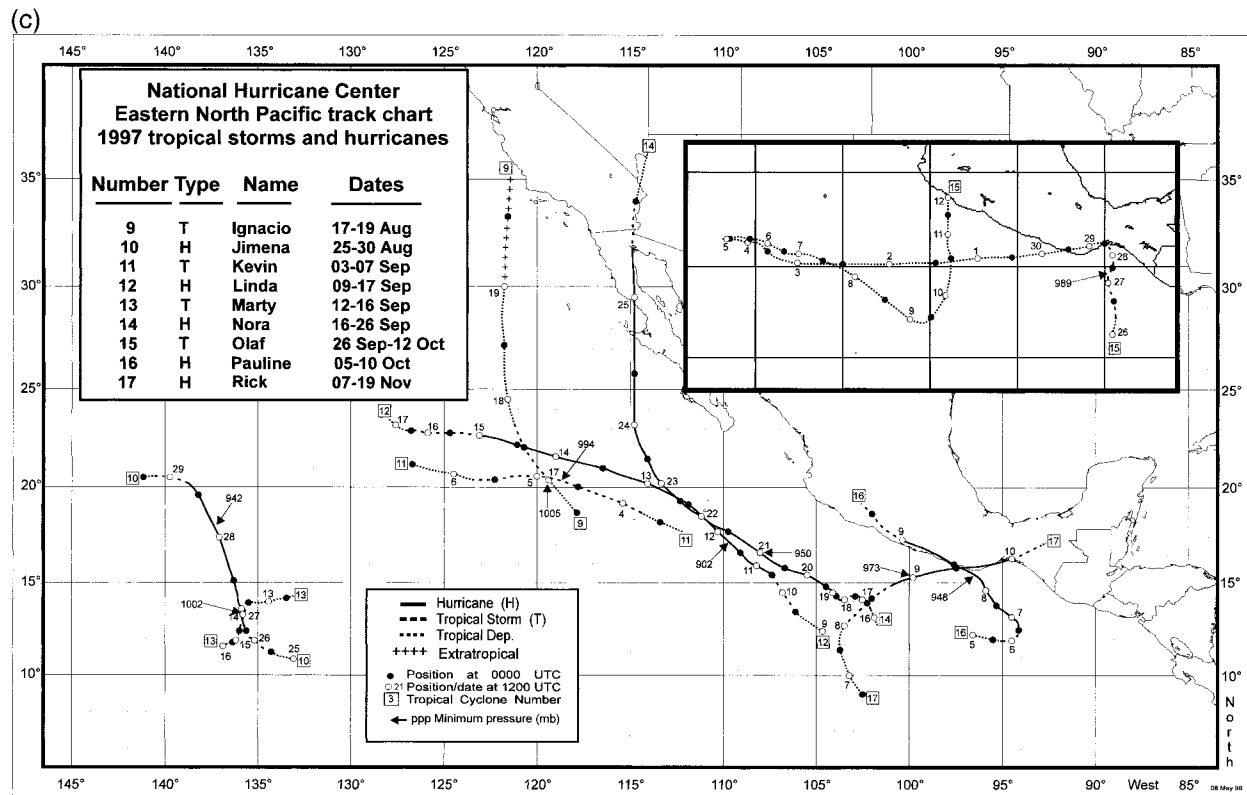


FIG. 1. (Continued)

in the Nicaragua municipalities of Chinandega, Corinto, El Realejo, and El Viejo.

b. Tropical Storm Blanca, 9–12 June

A broad area of cyclonic low-level westerly flow became established over the Pacific east of 100°W while Tropical Storm Andres was near the coast of El Salvador. A tropical disturbance grew within this perturbed environment and developed into a tropical depression in the Gulf of Tehuantepec at 1800 UTC 9 June. Under an upper-level ridge and over a warm ocean, the depression quickly became Tropical Storm Blanca. Initially, Blanca moved west-northwestward toward the coast of Mexico. However, a strong midlevel ridge over northern Mexico later steered the storm westward away from the coast.

Blanca reached its estimated maximum intensity of 40 kt and a minimum pressure of 1002 mb at 0000 UTC 11 June, based on an appearance of good outflow and some banding features on geostationary satellite imagery. However, surface observations indicated that Blanca's circulation was not well defined and Special

Sensor Microwave/Imager 85-GHz images showed that the tropical cyclone was quite small.

Soon thereafter, a weakening process began. Satellite and surface data suggested that the system no longer had a closed circulation at 1200 UTC 12 June.

Initially, most of the guidance models and the official forecast indicated a west-northwest track toward the coast of Mexico. This prompted a tropical storm warning for a portion of Mexico from Puerto Angel to Acapulco at 0300 UTC 10 June. Warnings were discontinued the next day when Blanca turned westward away from the coast.

c. Tropical Storm Carlos, 25–28 June

Satellite imagery showed an increase in cloudiness and thunderstorms over a broad area located several hundred miles off the southwest coast of Mexico on 22 June. Based on continuity, this disturbance may have originated from a tropical wave that moved from Africa to the eastern Atlantic Ocean on 8 June. The wave was very poorly defined on satellite imagery for several days while it passed over the Caribbean and Central America.

←

FIG. 1. Eastern North Pacific basin track chart for 1997: (a) storm numbers 1–8, (b) full track of storm number 7, and (c) storm numbers 9–17.

Intermittent signs of a low-level circulation were seen on 23 and 24 June. Deep convection became more concentrated and a tropical depression formed from the disturbance near 0600 UTC 25 June, while centered about 450 n mi south-southeast of the southern tip of Baja California. The developing cyclone moved toward the northwest near 10 kt.

The tropical depression strengthened into Tropical Storm Carlos by 1800 UTC 25 June as upper-level outflow became better established and convective banding increased. A minimum central pressure of 996 mb and maximum winds of 45 kt are estimated to have occurred near 0600 UTC 26 June. At this time, the cyclone was centered about 40 n mi south-southwest of Socorro Island, which was about its closest position to the island.

Convective activity soon diminished as Carlos moved over cooler water. Upper-level shear increased and by 27 June the low-level center was exposed from the convection. The movement of the tropical cyclone had become more westerly by this time in response to the low-level steering. Carlos weakened to a tropical depression near 0600 UTC 27 June when only minimal deep convection remained. It then dissipated by 0600 UTC 28 June about 500 n mi west-southwest of the southern tip of Baja California, although a weak swirl in the low clouds persisted for another day or so.

The lowest surface pressure reported from Socorro Island was 1001.1 mb at 0700 UTC 26 July, at which time maximum sustained winds were measured at 35 kt with gusts to 53 kt.

d. Hurricane Dolores, 5–12 July

Hurricane Dolores formed from a disturbance of uncertain origin. The development might have been related to a tropical wave that traversed the Atlantic Ocean from 17–26 June and moved slowly westward over the eastern North Pacific Ocean during the following week. On 3 and 4 July, clouds increased in the vicinity of the wave. The cloudiness was initially elongated from north to south, but some circular symmetry was noted by the end of the day on 4 July. Ship data indicated that surface pressures in the area were a little lower than usual, near 1005 mb, at that time. The first signs of a low-level circulation were noted early on 5 July.

Deep convective banding quickly increased in an environment characterized by upper-level diffluence. It is estimated that the disturbance became a tropical depression at 1200 UTC 5 July, about 600 n mi to the south of the southern tip of Baja California.

With a strong deep ridge to the north, Dolores moved toward 280°–290° at 10–15 kt for most of the cyclone's lifetime. Despite some northeasterly wind shear, the initial pace of development continued for about a day, during which time the cyclone became Tropical Storm Dolores and winds increased to 45 kt. The cyclone was then generating convection with cloud-top temperatures lower than -80°C . After a pause in development,

strengthening resumed on 7 July as the outflow became more symmetrical. Dolores became a hurricane that day and developed a mostly cloud-filled, ragged-appearing eye, analyzed from satellite images to be 10–20 n mi in diameter by the Air Force Global Weather Center. The hurricane attained its peak strength of 80 kt around 0600 UTC on 9 July, shortly after moving near 125°W.

The eye then disappeared and the cyclone gradually weakened while becoming sheared from the southwest and moving over progressively cooler waters from 9 to 11 July. Only a few clusters of deep convection were observed on 10 and 11 July. Dolores crossed 140°W and entered the central Pacific hurricane basin as a tropical depression on 11 July and dissipated the next day.

e. Hurricane Enrique, 12–16 July

A tropical wave crossed Dakar, Senegal, on 26 June, accompanied by a few clusters of deep convection and a well-defined low-level circulation as indicated by soundings from that site. As soon as the wave moved over the tropical Atlantic Ocean, it lost most of the convection and remained as a westward-moving weak synoptic feature for about 2 weeks. The wave crossed Central America during 6 and 7 July. On 8 July, a broad low-level circulation began to form south of the Gulf of Tehuantepec. It took three more days for the thunderstorms and the circulation to consolidate. It became a tropical depression near 0600 UTC 12 July, about 850 n mi south-southwest of the southern tip of Baja California.

Once the convection clustered near the center, the depression intensified rapidly and became a hurricane by 1200 UTC 13 July. Enrique moved between west-northwestward and northwestward around the periphery of a high pressure system. During that period, Enrique experienced some fluctuations in intensity. The eye became an intermittent feature and these fluctuations were represented by the increasing and decreasing of both objective and subjective Dvorak T-numbers (Dvorak 1984). It is estimated that the peak intensity of 100 kt and a minimum pressure of 960 mb occurred at 1800 UTC 14 July. Thereafter, the outflow became asymmetric and a weakening process began. It is estimated that Enrique was dissipating by 1800 UTC 16 July, when it became a swirl of low clouds moving over cool waters.

f. Hurricane Felicia, 14–22 July

The first indication of Hurricane Felicia was the detection of a large area of increasing thunderstorms centered several hundred miles south of Manzanillo, Mexico, on 13 July. On 14 July, this disturbed weather became better organized with a banding-type cloud pattern and developed into a tropical depression. Felicia's movement during its existence was toward the west-northwest at forward speeds varying from 5 to 15 kt.

For the first day or so, there was little additional de-

velopment as the depression experienced northeasterly wind shear, partially associated with the outflow from Hurricane Enrique. However, on 15 July, the system was upgraded to Tropical Storm Felicia as Enrique's outflow retreated. A burst of deep convection on 16 July was evidence of further development and Felicia became a hurricane on 17 July when there was a suggestion of the formation of an eye between two interlocking convective bands. Felicia then leveled off as a 65-kt hurricane for 24 h under northwesterly shear caused by a nearby upper-level trough.

On 18 July, an eye became better defined and a period of intensification began that culminated with estimated 115-kt sustained wind speeds on 19 July. The hurricane's maximum wind speed remained 115 kt for most of 19 July and then began a continuous decrease as a result of colder SST and a hostile synoptic environment caused by another approaching upper-level trough.

Felicia moved west of 140°W on 21 July and was reduced to a swirl of low clouds on 22 July in the central Pacific Ocean.

g. Hurricane Guillermo, 30 July–15 August

Rawinsonde data from Dakar indicated that a well-defined tropical wave emerged from the west coast of Africa on 16 July. The wave was tracked across the Atlantic in satellite imagery, although associated deep convection was minimal. Strong westerly winds aloft made tracking the wave difficult as it crossed the Caribbean. However, extrapolation would place the wave in the vicinity of increased cloudiness and convection off the Pacific coast of Central America on 27 and 28 July. Evidence of a poorly defined cloud system center within a somewhat isolated tropical disturbance appeared in satellite imagery on 29 July. Convective banding increased as a broad cyclonic circulation became established. A tropical depression formed from the disturbance near 1200 UTC 30 July while centered about 300 n mi south of Salina Cruz, Mexico. The tropical cyclone moved west-northwestward at 10–15 kt in response to a deep-layer-mean ridge to its north.

Deep convection became concentrated near the circulation center and the depression strengthened into Tropical Storm Guillermo at 0600 UTC 31 July while centered about 325 n mi to the south-southeast of Acapulco, Mexico. A well-defined central dense overcast developed over the circulation center and Guillermo became a hurricane at 1800 UTC 1 August while centered about 300 n mi southwest of Acapulco. Upper-level outflow became well established, and an eye appeared in satellite imagery on 2 August. Strengthening continued and it is estimated that Guillermo reached its peak intensity with 1-min surface wind speeds of 140 kt and 919-mb minimum central pressure near 0000 UTC 5 August while centered about 700 n mi to the southwest of the southern tip of Baja California. Shortly thereafter, infrared satellite imagery showed that cloud-top tem-

peratures surrounding the eye gradually warmed, although the eye remained visible until 7 August.

Guillermo moved over cooler water and weakened to a tropical storm by 0600 UTC 8 August while centered about 1100 n mi east of Hawaii. It passed 140°W into the central Pacific basin just after 1800 UTC 9 August. Then the low- to midlevel flow turned the weakening cyclone more toward the north-northwest around the western periphery of the subtropical ridge. Guillermo weakened to a tropical depression at 1800 UTC 10 August but regained tropical storm strength about 24 h later. The storm temporarily turned more toward the west-northwest and passed about 700 n mi to the north-east of the Hawaiian Islands on 13 August.

Guillermo again weakened to a tropical depression at 1200 UTC 15 August and became extratropical near 0000 UTC 16 August. The extratropical low recurved across the North Pacific, moving to a position about 500 n mi west of Vancouver Island, British Columbia, on 19 August. The low persisted for a few days longer, slowly moving to within 300 n mi of the coast of northern California before being absorbed by a larger extratropical cyclone on 24 August.

Best-track records show Hurricane Linda in September 1997 with maximum sustained winds of 160 kt and Hurricane Ava in 1973 with maximum sustained winds of 140 kt. Since 1966, these are the only eastern Pacific hurricanes on record with winds as strong as, or stronger than, Guillermo.

Aircraft reconnaissance data were provided by the National Oceanic and Atmospheric Administration (NOAA) Hurricane Research Division from P-3 aircraft conducting a vortex motion and evolution experiment on 2 and 3 August. Several global positioning system (GPS) dropwindsondes were released from the 700-mb level within the eyewall of Guillermo. For the first time, wind data with relatively high vertical resolution were measured and reported from flight level all the way down to within a few meters of the surface within the eyewall of a major hurricane. Profiles of wind speed versus altitude showed considerable variations among the individual "drops." A figure showing a profile from one of the GPS sondes dropped within the eyewall of Hurricane Erika is presented in the companion Atlantic hurricane season summary in this journal. GPS sonde data are expected to improve our understanding of the vertical structure of the wind field in and around a tropical cyclone.

h. Tropical Storm Hilda, 9–15 August

Hilda may be traced back to a tropical wave that departed western Africa on 26 July. Although the wave did spawn a cluster of convection northeast of Puerto Rico on 31 July, this system generally remained nondescript during its passage across the tropical Atlantic, the Caribbean, and then across Central America on 3–4 August. Convection associated with the wave in-

creased to the southwest of the Gulf of Tehuantepec on 5 July. A cloud circulation center was evident on 7 August. The cloud pattern became better organized on 9 August, as convection became more consolidated and curved cloud bands were discernible. The system became a tropical depression around 0000 UTC 10 August about 920 n mi south-southwest of the southern tip of Baja California.

The depression strengthened to a storm on 11 August and reached its peak intensity of 45 kt on 12 August. Southerly shear caused weakening on 13 August and Hilda dissipated on 15 August. The tropical cyclone moved on a generally northward course throughout its five days of existence.

i. Tropical Storm Ignacio, 17–19 August

Tropical Storm Ignacio formed from a large area of disturbed weather that persisted well west of mainland Mexico from 14–16 August. There were at least three different centers of activity within the weather system during that period. The disturbance that became Ignacio was first analyzed early on 16 August, several hundred miles to the southwest of the southern tip of Baja California. By 1800 UTC 16 August, convective bands had developed and they were turning cyclonically around a midlevel cloud system center. Animation of visible satellite pictures indicated that low clouds were not as well organized. The system continued to become better organized, however, and it is estimated that it became a tropical depression at 0000 UTC on the 17th, about 450 n mi to the southwest of Cabo San Lucas.

The genesis occurred to the northwest of the area where most eastern North Pacific tropical cyclones form, just south of that basin's sharp gradient in SST, and also to the south of a midlevel to upper-level low centered offshore of southern California. A trough trailed southwestward from the low and the steering currents associated with the low and trough moved the tropical cyclone toward the northwest and then the north at 10–15 kt from 17 through 19 August.

The most intense burst of deep convection near the cyclone's center occurred early on 17 August and satellite intensity estimates reached 35 kt at 1200 UTC. The strengthening trend was short-lived. Ignacio moved over much cooler waters and encountered southerly shear. In that environment, deep convection was sustained only intermittently in the northwest quadrant, and Ignacio weakened back to a tropical depression early on 18 August.

Satellite pictures indicated a rejuvenation of cold cloud tops, mostly in the cyclone's northern semicircle on 19 August. This development was likely induced by baroclinic processes, occurring over relatively cool waters where a midlatitude trough was approaching from the northwest. These observations form the basis for designating the system as extratropical at 1200 UTC 19

August. The extratropical low dissipated near the south-central California coast about 24 h later.

Clouds and precipitation associated with the remnant circulation aloft moved northward on 19 and 20 August, through northern California, Oregon, Washington, and southern British Columbia. On 20 August, this moisture was incorporated into the eastern part of a large offshore extratropical cyclone associated with the remnant of Hurricane Guillermo.

Rainfall totals ranged from 10 to 30 mm over coastal areas of central California. A maximum of 55.1 mm was recorded at Three Peaks in the coast range about 100 n mi south of San Francisco. Such rains are rare events in the summer months in California. About 25 mm of rain fell in San Francisco, and that was more than had previously occurred there for the entire month of August since records began in 1850. There were no reports of casualties or damages from this rain but it was reported that thunderstorms were responsible for some power outages in central California.

j. Hurricane Jimena, 25–30 August

Jimena developed from a large area of disturbed weather centered near 130°W, where SSTs were 1.0°–1.5°C above normal. Initially, the disturbance was under an unfavorable upper-level westerly wind environment. The convection increased and an upper-level anticyclone gradually built over the system. A tropical depression formed within this area of weather at 1200 UTC 25 August. After becoming a tropical storm by 0000 UTC 26 August, Jimena intensified rapidly and developed an eye. The estimated winds increased from 65 kt to 115 kt in about 15 h on 27 August. Jimena's maximum winds were estimated near 115 kt for 36 h and peaked at 120 kt at 1500 UTC 28 August.

Jimena was moving on a north-northwesterly track when a strong upper-level trough moved by and sheared the hurricane. Jimena weakened as fast as it developed. Wind estimates decreased from 115 to 30 kt in about 24 h. The remaining low-level circulation center moved westward into the central Pacific basin on 29 August. It dissipated by 0000 UTC 30 August.

k. Tropical Storm Kevin, 3–7 September

Kevin may have originated from a tropical wave that moved from Africa to the eastern tropical Atlantic Ocean on 16 August. The wave remained weak as it moved across the Atlantic at low latitudes and then across northern South America. On 26 August, convection flared up just south of Panama in association with the wave. The convection developed and dissipated intermittently for the next several days as the system moved near and parallel to the Pacific coast of southern Mexico.

Although satellite Dvorak classifications began on 1 September, it was not until 3 September that satellite

imagery indicated a well-defined low-level circulation, along with a small circular area of deep convection near the center and a band of convection to the east. Tropical depression status began at 1800 UTC on 3 September while the system was centered about 325 n mi south-southwest of the southern tip of Baja California.

The area of deep convection over the center became larger and outflow aloft became better defined. It is estimated that Kevin reached tropical storm strength at 0600 UTC on 4 September and a maximum intensity of 50 kt at 0000 UTC on 5 September. Only 18 h later, at 1800 UTC, the center of the storm was devoid of deep convection. By 0600 UTC on 6 September, Kevin weakened to a depression and was reduced to a swirl of low clouds 24 h later. Kevin's motion was basically toward the west-northwest at about 12 kt from the time it became a depression, as it was steered by a ridge to its north. Late on 5 September, Kevin began to weaken and became decoupled from upper-layer flow. The system moved westward until dissipation on 7 September.

The ship *Kentucky Highway* reported a 39-kt sustained wind speed at 1800 UTC on 4 September while located about 110 n mi east-northeast of the storm center.

l. Hurricane Linda, 9–17 September

Linda is estimated from satellite imagery to be the strongest hurricane on record in the eastern Pacific.

Rawinsonde data from Dakar indicated that a well-defined tropical wave emerged from the west coast of Africa on 24 August. The wave was tracked across the Atlantic and the Caribbean Sea and increased cloudiness and convection off the Pacific coast of Panama on 6 September was likely associated with the wave. Evidence of a poorly defined cloud system center within a broad tropical disturbance appeared in satellite imagery early on 9 September. A banding-type pattern emerged, and a tropical depression formed from the disturbance near 1200 UTC 9 September while centered about 400 n mi south of Manzanillo, Mexico. The tropical cyclone moved northwestward at 5–10 kt, partly in response to a mid- to upper-level low in the vicinity of lower Baja California.

Deep convective banding increased and the depression strengthened into Tropical Storm Linda at 0000 UTC 10 September. Upper-level outflow became very well established and intermittent hints of an eye appeared by 0000 UTC 11 September, at which time Linda is estimated to have become a hurricane. Rapid strengthening occurred and it is estimated that Linda reached its peak intensity of 160 kt winds and 902-mb minimum central pressure near 0600 UTC 12 September while centered about 125 n mi southeast of Socorro Island. A small, well-defined eye embedded within very cold convective tops was visible on satellite imagery at this time, as shown in Fig. 2. Several hours later, the center moved

very close to Socorro Island, and Fig. 3 shows a visible satellite image of the eye approaching this island.

On 13 September, Linda began moving toward the west-northwest at 10–12 kt in response to a building ridge to the north of the tropical cyclone. Linda moved over cooler water and weakened to a tropical storm by 1200 UTC 15 September while centered about 730 n mi west of the southern tip of Baja California. Steering currents also began weakening about this time and the forward motion gradually decreased to near 5 kt. Linda, far from land, weakened to a tropical depression by 0600 UTC 17 September and dissipated by 0000 UTC 18 September. However, a weakening swirl of mostly low clouds persisted for a few more days.

Objective Dvorak T-numbers were calculated at 30-min intervals. These objective Dvorak T-numbers ranged between 7.5 (155 kt) and 8.0 (170 kt) from 0000 UTC 12 September to 1200 UTC 12 September. Maximum subjective T-numbers also ranged between 7.5 and 8.0. The 160-kt peak intensity of Linda, estimated to have occurred near 0600 UTC 12 September, is a conservative estimate that is 10 kt lower than the maximum objective or subjective T-numbers.

A maximum 1-min sustained wind speed of 160 kt (and corresponding minimum central pressure of 902 m) makes Linda the strongest hurricane in the eastern Pacific since records began in 1949.

The NOAA high-altitude jet flew synoptic-flow dropwindsonde missions on 14 and 15 September. This provided additional data for the 0000 UTC global model runs on those days. Also, four vortex fixes were provided from a U.S. Air Force Reserve (Hurricane Hunter) aircraft on 14 September.

Because of a power failure, observations were not taken at Socorro Island during the time that hurricane conditions are expected to have occurred.

Some of the track guidance computer models initialized after 0000 UTC 13 September indicated recurvature toward Baja California or southern California. An experimental 5-day Geophysical Fluid Dynamics Laboratory model forecast indicated a weakening tropical cyclone centered just off the southern California coast at the verifying time of 0000 UTC 18 September. A few of the official forecasts also indicated recurvature on 13 and 14 September. The best track shows that recurvature did not occur.

m. Tropical Storm Marty, 12–16 September

Marty's origins are associated with two westward-traveling tropical waves. The first wave crossed Central America around the end of August and another entered the eastern Pacific about 3 days later. These two waves appeared to contribute to an area of disturbed weather that was located near 15°N, 129°W on 10 September. Deep convection associated with the system increased in a "bursting"-type event on the 11th, but there was no significant increase in organization until the follow-

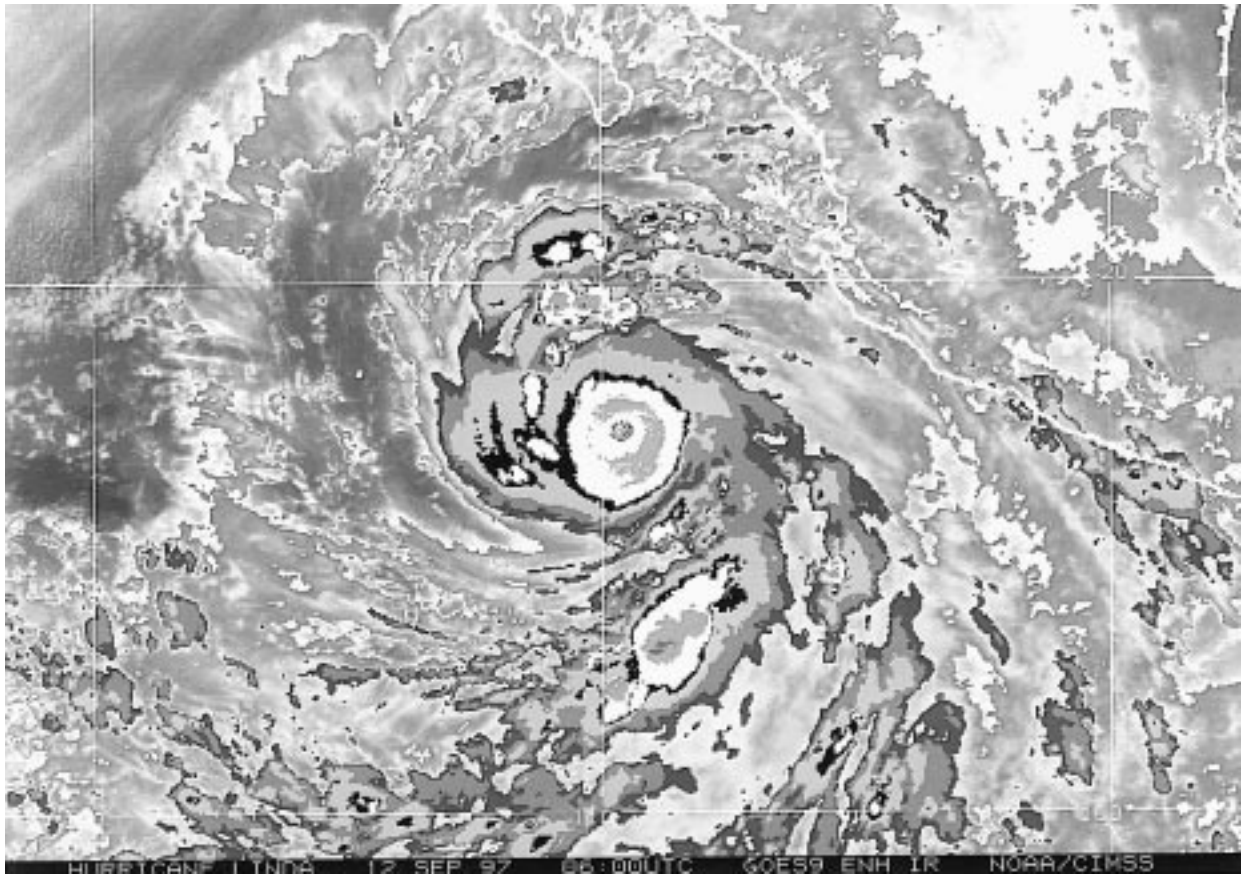


FIG. 2. GOES-9 enhanced infrared satellite image of Hurricane Linda at 0600 UTC 12 September 1997. The maximum 1-min wind speed is estimated at 160 kt at this time.

ing day, when curved cloud bands became readily apparent. The system is estimated to have become a tropical depression at 1800 UTC 12 September. The depression was centered about 1300 n mi east-southeast of the island of Hawaii at that time.

Steering currents were weak and the system never moved faster than 5 or 6 kt. The depression moved a little south of due westward on 12 and 13 September, and, after strengthening into Tropical Storm Marty around 0000 UTC on 14 September, it turned southwestward and then southward. Marty's forward speed slowed to a crawl on 15 September, and it weakened back to a depression that day. The weakening was apparently caused by vertical shear due to upper-level southeasterly flow over the area with the low-cloud center becoming clearly exposed. Strong shearing continued, weakening the slow-moving Marty to dissipation by 1800 UTC 16 September.

n. Hurricane Nora, 16–26 September

Hurricane Nora formed early on 16 September about 250 n mi to the southwest of Acapulco. It originated in a large area of disturbed weather that had slowly become

organized while drifting west-northwestward during the previous few days. This activity was likely related to a westward-moving tropical wave that crossed from Africa into the Atlantic on 30 and 31 August. The northern part of the wave was associated with the formation of Hurricane Erika in the central tropical Atlantic. At the same time, the southern part continued westward through the Caribbean Sea and northern South America, and arrived in the eastern Pacific basin on 12 September.

Nora developed in an environment of relatively light wind shear and over warm SST of 29°–30°C. Deep convection quickly increased and became organized in well-defined bands on 16 September and the system became a tropical storm at 1800 UTC. Further strengthening occurred over the following 2 days. The first signs of what would become a rather large and ragged eye were detected in infrared satellite pictures early on 18 September. By late that day, Nora was a hurricane with 90-kt sustained winds.

During Nora's first few days, the winds around a mid-level high over northern Mexico helped direct the tropical cyclone slowly toward the west-northwest. From midday on 18 September to early on 20 September, however, Nora nearly stalled. The hurricane weakened

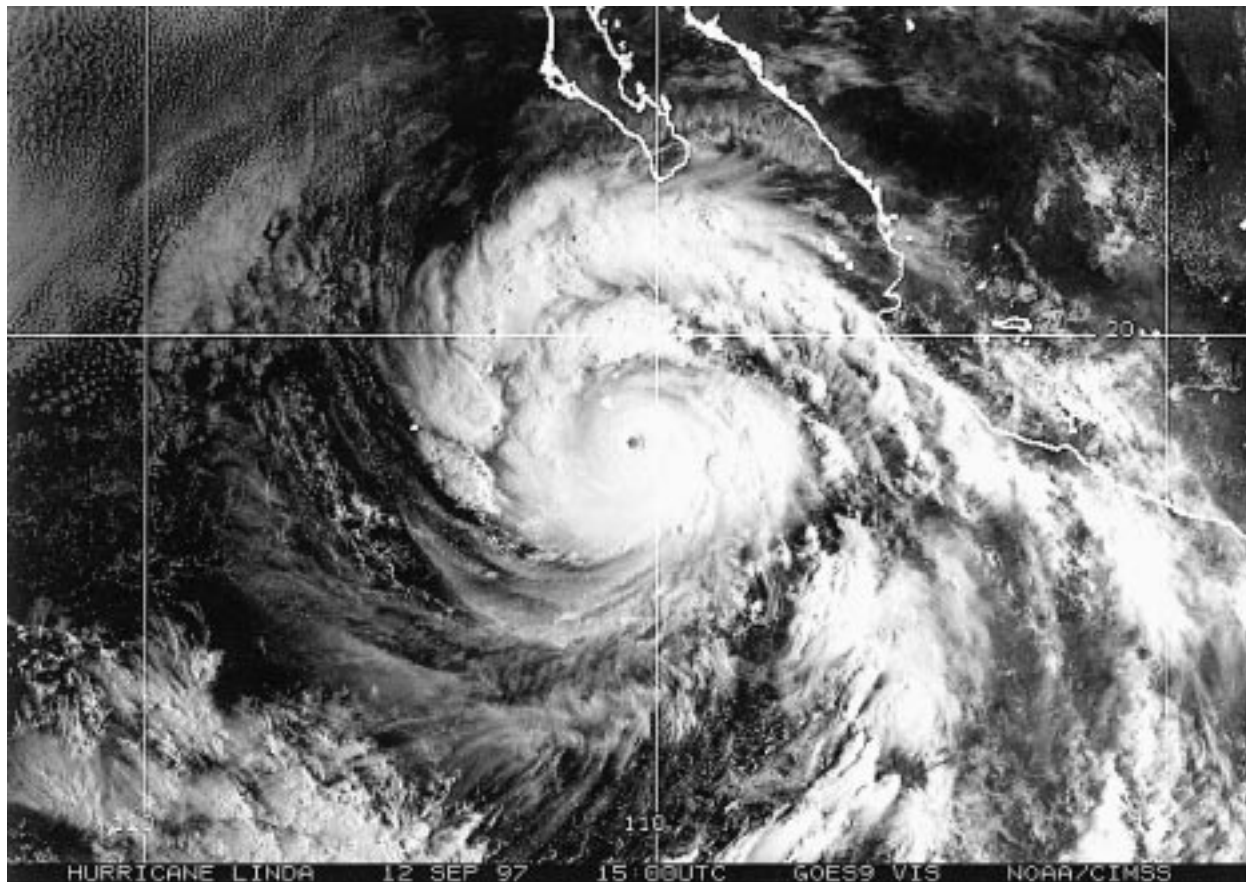


FIG. 3. GOES-9 visible satellite image of Hurricane Linda at 1500 UTC 12 September 1997. The maximum 1-min wind speed is estimated at 150–155 kt at this time.

during that period. Convection decreased and the eye disappeared. The maximum wind speed is estimated to have decreased to 65 kt. This weakening may have been related to the hurricane's prolonged stay over waters cooled by upwelling beneath its circulation. Analyses in this part of Nora's wake show SSTs cooled by about 2°C, on average, to about 27°C.

By late on 20 September, Nora was on the move again, at 5–10 kt toward the west-northwest or northwest, roughly parallel to the southwest coast of Mexico. Nora then rapidly restrengthened. The eye reappeared, initially with a diameter of 15 n mi, and cloud tops cooled. Nora reached its peak maximum wind speed of 115 kt near 1200 UTC on 21 September.

On 21–23 September, Nora's track converged with, and then followed, the track previously taken by Hurricane Linda. In that area, Linda's extremely strong circulation had induced lower SSTs. Nora gradually weakened over Linda's wake, with the eye temporarily broadening to a diameter of about 50 n mi and the eyewall becoming broken. Estimated wind speeds decreased to about 70 kt at 1800 UTC on 23 September.

An omega-like blocking pattern developed over the western United States during the last week of September.

This left a weakness in the height pattern to the north of Nora and eventually a trough with a cutoff low to the northwest of the hurricane. The track of Nora became north-northwestward and then northward on 24 September. This carried Nora over yet another SST anomaly, a large patch of waters more than 2°C above normal near the west coast of Baja California. Nora remained over waters of at least 26°C all the way to its landfall on the morning of 25 September at Punta Eugenia and then again several hours later about 50 n mi south-southeast of San Fernando, Baja California. It was still at hurricane strength during its landfalls.

Nora was accelerating northward at landfall, steered by the flow associated with the trough to its northwest. The center of the cyclone crossed the Baja California peninsula at 20–25 kt and traveled up the western shoreline of the Gulf of California. It crossed into the United States, near the California–Arizona border, still as a tropical storm, near 2100 UTC on 25 September. Most of the heaviest precipitation was then located to the northeast of the center.

Rapid weakening ensued and winds dropped to tropical depression strength near 0000 UTC on 26 September, when the center was located about midway between

Blythe and Needles, California. The low-level center was moving toward the north-northeast as it degenerated early on 26 September. A remnant circulation aloft persisted, however, and is likely to have been responsible for a period of near hurricane-force winds observed by the National Weather Service (NWS) Cedar City Doppler radar, located in the mountains of southwestern Utah at an elevation of about 3230 m.

The residual area of cloudiness and showers gradually became more diffuse over the following 2 days while moving generally northeastward, through portions of Utah, Colorado, Idaho, and Wyoming.

A 39-kt 2-min sustained wind was observed at Yuma during Nora's passage. Such observations of tropical storm force winds are a rarity in the United States for eastern Pacific tropical cyclones. The peak gust observed at Yuma was 47 kt. A gust to 45 kt occurred at Ajo, Arizona.

The NWS Doppler radar at Yuma showed a 40 n mi wide band of hurricane force winds aloft to the east of Nora's center near the Arizona–Sonora border near noon local time on 25 September. These winds were observed at about 4000–5000 ft and were likely related to the patch of near-hurricane force winds observed over the high terrain of southwestern Utah 12–18 h later.

The Yuma radar indicated a small area with near 250 mm of rain along the northern Gulf of California coast of Baja California. In the United States, the 304 mm recorded at the 5700-ft level in the Harquahala Mountains in Arizona was, by far, the largest total. More than 75 mm occurred in some spots in Arizona, California, Nevada, and Utah. Some of the amounts were comparable to the local yearly average rainfall.

Two deaths were reported from Mexico in association with Nora. One person was electrocuted by a downed power line in Mexicali. The other fatality occurred to a diver caught in strong underwater currents created by Nora off the coast of the San Quintin Valley. In the United States, there were no deaths directly related to Nora. The California Highway Patrol attributed three or four traffic fatalities in southern California to weather.

Although Nora remained well offshore from southwestern mainland Mexico, the Associated Press reported that waves to near 5 m hit that coastline, destroying dozens of homes. It also destroyed the Pie de la Cuesta beaches of Acapulco.

About 350–400 people were made homeless by floodwater in the town of Arroyo de Santa Catarina in northern Baja California. Heavy damage and flooding were reported in San Felipe, on the northwestern shore of the Gulf of California. There was significant wind damage on the northeastern shore, at Puerto Peñasco, and waves of near 3 m were reported there.

Damage totals in the United States are in the several hundred million dollar range based on media reports of agricultural losses.

In Somerton, Arizona, 10 miles south of Yuma, dam-

age to mobile homes and flooding were reported. About 12 000 people lost power in Yuma.

In California, about 125 000 people lost power in the Los Angeles area with scattered, much smaller outages elsewhere. In San Diego, El Centro, Palm Springs, and Indio, street flooding was reported. Winds knocked down about 16 power poles in Seeley.

The remnant circulation aloft apparently downed and/or sheared off the tops of hundreds of large (1–2-ft diameter) trees in southwestern Utah, mainly at elevations above 3000 m in the area that includes the Dixie National Forest.

o. Tropical Storm Olaf, 26 September–12 October

Olaf was a tenacious tropical cyclone that persisted for a couple of weeks despite a prevailing unfavorable upper-level environment.

Olaf appears to have developed from an area of disturbed weather associated with a tropical wave that crossed Central America on 22 September and then slowly moved westward over the eastern Pacific Ocean. The disturbance became nearly stationary while the shower activity gradually increased. During that time, there was a strong upper-level low over the Gulf of Mexico that moved southwest into the eastern Pacific, to the west of the disturbance. Initially, the strong upper-level winds associated with the low produced a shearing environment. However, the disturbance gradually developed an upper-level outflow, resulting in the formation of a tropical depression near 1200 UTC 26 September, about 300 n mi south of the Gulf of Tehuantepec. It became Tropical Storm Olaf a few hours later.

The upper low steered the tropical cyclone slowly northward toward the southeastern coast of Mexico. During that period, satellite intensity estimates and ship reports indicated that Olaf was strengthening. Olaf reached estimated maximum winds of 60 kt and a minimum pressure of 987 mb at 1800 UTC 27 September. Thereafter, a portion of the circulation began to interact with mountainous terrain and Olaf gradually weakened. It was a tropical depression when the center reached the coast in the vicinity of Salina Cruz at 0000 UTC 29 September. A few hours later, over land, the circulation was not identifiable. However the remnants moved back over water and were tracked to a few hundred miles southwest of the southern tip of Baja California by 5 October.

The depression moved toward the southeast on 8 October, embedded within a much larger cyclonic circulation. The depression then moved toward the north and made its final landfall near Manzanillo, Mexico, on 12 October. It weakened over the high terrain, but the remnant cloudiness and showers again moved back over water, where it failed to redevelop.

Ship *OUIH2* was near Olaf for several hours and it was able to send a few valuable observations. The vessel reported maximum winds of 55 kt and a minimum pres-

sure of 1003.5 mb at 0300 UTC 27 September when it was located just west of the center of Olaf. This observation was used to estimate the maximum intensity of Olaf.

Strong winds and heavy rains associated with Olaf bashed Mexico's Pacific south coast. Media reports said that military and government officials from Mexico were searching for three fishing vessels missing off the coast of Acapulco. Heavy rains also affected Guatemala and El Salvador where floods were reported. There are no reports of damage associated with Olaf's second landfall.

p. Hurricane Pauline, 5–10 October

Pauline dumped up to 400 mm of rain along the south coast of Mexico and was responsible for an estimated 230 (or more) deaths in the states of Oaxaca and Guerrero.

Pauline may have developed from a tropical wave that moved from Africa to the eastern tropical Atlantic Ocean on 16 September. The southern portion of this wave moved across northern South America and then over the eastern Pacific Ocean near Panama about 10 days later. By 3 October, a weak lower-tropospheric trough from the northwestern Caribbean Sea had developed southwestward across southeast Mexico and northern Central America and disrupted the normally westward steering currents in this area. By 3 October, the wave developed a distinct area of convection and began to drift eastward. On 5 October, a well-defined low-level circulation formed and tropical depression status began about 200 n mi south of Puerto Angel, Mexico.

With an absence of vertical shear and the appearance of convective banding features and a small central dense overcast, the system gradually strengthened to a tropical storm early on 6 October. Hurricane status was reached later that day when satellite imagery showed a hint of an eye feature. This was soon followed by the appearance of a small well-defined eye and rapid intensification.

A strong high pressure system over the southeastern United States eroded the trough over southeastern Mexico and Pauline gradually turned toward the northwest on 6–8 October while continuing to intensify. Pauline reached a peak intensity of 115 kt on 7 October, weakened slightly, and again reached 115 kt on 8 October. By 8 October, the center of the hurricane was close to the coast of Mexico near Puerto Angel and interaction of the northern half of the circulation with the high terrain of Mexico resulted in weakening.

The center crossed the coast at about 0000 UTC 9 October near Puerto Escondido with sustained winds estimated at 95 kt. It then turned toward the northwest and accelerated. Figure 4 is a satellite image of Pauline about 6 h after landfall. Pauline moved nearly parallel to the coast for about 24 hours while continuing to weak-

en. Pauline dissipated by 1200 UTC 10 October over the state of Jalisco near Tuxpan.

Only limited surface reports have been received from Mexico. The ship *Rijndam*, located about 120 n mi northeast of the center at 0600 UTC 7 October, reported sustained winds of 51 kt. A report of 30 kt with gusts to 60 kt was received from Puerto Escondido at 2145 UTC 8 October and there were no reports available after this time. Acapulco did report continuously while the center was nearby and the maximum wind from there was 40 kt with gusts to 51 at 0745 UTC 9 October. Based on satellite intensity estimates, sustained winds of 115 kt may have affected the coastline of the state of Oaxaca near Puerto Angel. But Acapulco's observations indicate that Pauline was barely of hurricane strength when it reached the Acapulco area and the primary effect to the state of Guerrero was the heavy rainfall, which also affected Oaxaca. Rainfall totals provided by the National Meteorological Service of Mexico show that 411.5 mm fell in the Acapulco area.

The associated heavy rainfall sent muddy flood waters over many communities. The hillside outskirts of Acapulco were particularly hard hit by flooding. Media reports put the death toll at 230 or more persons and hundreds of thousands were left homeless. Reuters reported that the Red Cross estimated the death toll at 400, but this has been disputed by Mexican officials.

Although winds up to 115 kt may have hit the coast in the Puerto Angel area, there have been no reports received that specifically describe the wind or storm surge damage, which may have been confined to a sparsely populated area.

q. Hurricane Rick, 7–10 November

Hurricane Rick made landfall in the state of Oaxaca, Mexico, as a category one hurricane on the Saffir–Simpson hurricane scale. This region was hit by Hurricane Pauline about 1 month earlier.

Satellite imagery showed an increase in cloudiness several hundred miles south of the Gulf of Tehuantepec on 5 November. This disturbance may have originated from a tropical wave that moved from Africa to the eastern Atlantic on 15 October. However, the wave was poorly defined on satellite imagery while it passed over much of the Atlantic and Caribbean. Therefore, continuity is the basis for relating the wave to Rick's origins.

The disturbance soon developed a distinct banding cloud pattern. Satellite classifications began at 0000 UTC 6 November, although the circulation center was poorly defined. The center became better organized and a tropical depression formed from the disturbance near 0000 UTC 7 November, while centered about 500 n mi south-southwest of Acapulco, Mexico.

The developing cyclone initially moved slowly toward the northwest. It then gradually turned toward the north in response to a deep-layer-mean trough to the northwest. Deep convection increased near the center

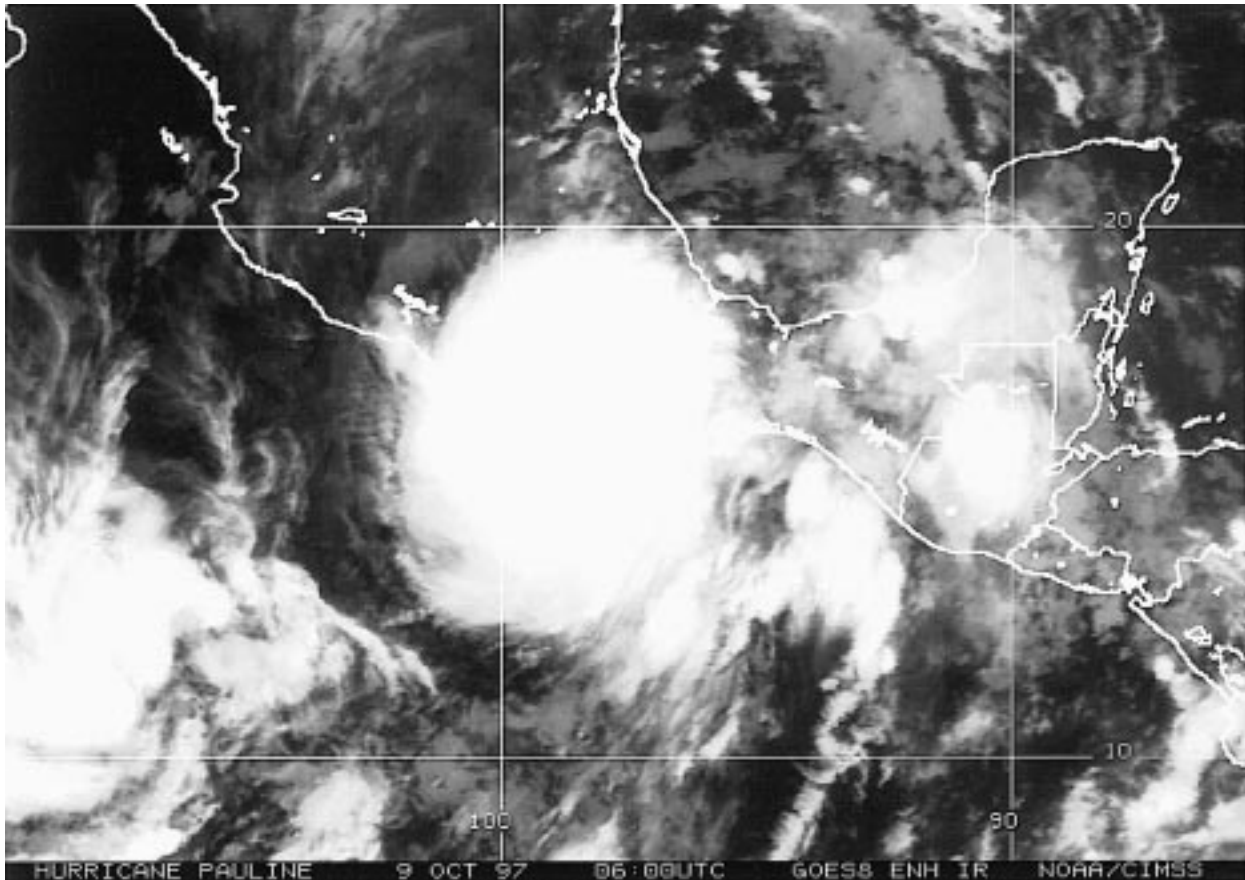


FIG. 4. GOES-8 enhanced infrared satellite image of Hurricane Pauline at 0600 UTC 9 October 1997. Pauline's center was on the coast at this time and the maximum 1-min wind speed is estimated at 70 kt.

and it is estimated that the depression strengthened into Tropical Storm Rick by 1200 UTC 8 November, while centered about 325 n mi southwest of Acapulco. A very cold central dense overcast developed as Rick became a hurricane at 0600 UTC 9 November. The hurricane was moving northeastward near 12 kt by this time. An eye appeared in satellite imagery and it is estimated that Rick reached its peak intensity of 85-kt winds near 1200 UTC 9 November, while centered about 100 n mi south of Acapulco. The radar from Acapulco showed the well-defined center of the hurricane moving east-northeastward until landfall in the vicinity of Puerto Escondido near 0100 UTC 10 November. The maximum sustained winds at landfall are estimated near 75 kt. Figure 5 is a satellite image of Rick near the time of landfall.

The center of the weakening tropical cyclone moved nearly parallel to the coastline of Mexico along the northern Gulf of Tehuantepec for another 12 h or so, eventually dissipating over the central portion of the state of Chiapas. The remnant of the cyclone was visible in satellite imagery as a weak low-level cloud swirl over the southeastern Bay of Campeche on 11 November, void of all deep convection.

The maximum sustained surface wind reported by the

Meteorological Service of Mexico from the point of landfall at Puerto Escondido, Mexico, was 65 kt at 0200 UTC 10 November. No eye was visible in geostationary satellite imagery for nearly 12 h before landfall, during which time radar data from Acapulco were invaluable in tracking the center.

About 250 mm of rain was reported at Puerto Escondido. Locally heavy rains likely occurred elsewhere over the states of Oaxaca and Chiapas.

There have been no reports of injuries or deaths related to Rick. The Associated Press reported downed trees and washed out roads in Oaxaca. Some of these roads had been recently repaired after Hurricane Pauline. The hurricane also knocked out communications in some small coastal villages.

3. Forecast verification

The NHC issues advisories every 6 h on all tropical cyclones in the Atlantic and eastern Pacific basins. These advisories include a 72-h forecast of track and intensity. A best-track track and intensity are determined for each tropical cyclone, after the fact, using all available information and are the basis for verifying the fore-

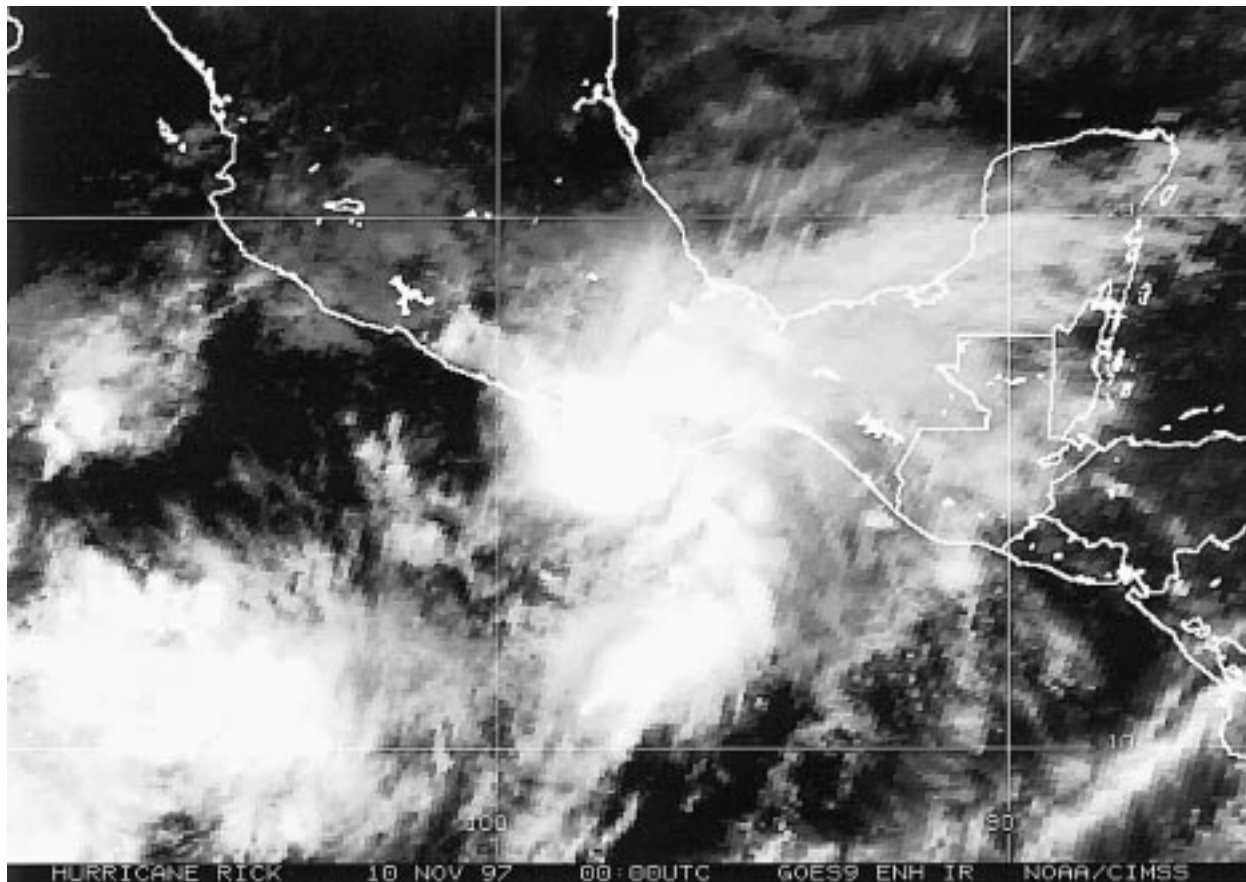


FIG. 5. GOES-9 enhanced infrared satellite image of Hurricane Rick at 0000 UTC 10 November 1997. Rick's center was near landfall at this time and the maximum 1-min wind speed is estimated at 75 kt.

casts. The track forecast error is defined as the great circle distance between a forecast position and a best-track position for the same time. The tracks shown in Fig. 1 are based on the best tracks. Two intensity forecast errors are defined. One is the bias, which is the algebraic difference between a forecast maximum 1-min wind speed and a best-track wind speed. The second is the absolute error, which is the absolute difference between the forecast and best-track wind speed.

Table 2 shows the average official NHC track forecast errors for 1997 for the eastern Pacific basin, along with the previous 10-yr averages and the CLIPER climato-

logical/persistence statistical track model average errors for comparison. The official average track forecast errors were slightly smaller than the previous 10-yr averages at all forecast periods except at 72 h where they were slightly larger. The CLIPER errors for 1997 were about the same as their previous 10-yr averages, suggesting that this year's tracks were near normal in terms of forecast difficulty.

Table 3 shows the average bias and average absolute official NHC wind speed errors for the eastern Pacific basin. In 1997, there was a negative bias at all forecast periods. The 1990–96 average official bias is also neg-

TABLE 2. A homogeneous comparison of official and CLIPER (climatology and persistence) track forecast errors (n mi). Error = the magnitude of the great circle distance between forecast and observed positions.

	Forecast period (h)					
	0	12	24	36	48	72
1997 average official error	10.9	35.8	66.8	98.0	129.9	208.4
1997 average CLIPER error	10.9	38.9	75.7	118.1	158.5	242.2
No. of cases	239	239	208	176	148	109
1987–96 average official error	12.9	38.8	71.3	105.3	138.1	194.3
1987–96 average CLIPER error	12.9	41.2	77.4	117.5	157.1	225.6
No. of cases	2293	2288	2058	1822	1607	1228

TABLE 3. A homogeneous comparison of official and SHIFOR (climatology and persistence) maximum 1-min wind speed forecast errors (kt). Error = forecast - observed. Absolute error = |forecast - observed|.

	Forecast period (h)					
	0	12	24	36	48	72
1997 average official error (bias)	-0.7	-1.4	-4.1	-5.5	-7.3	-4.4
1997 average absolute official error	3.8	9.5	15.9	19.4	22.1	23.0
1997 average SHIFOR error (bias)	-0.7	-1.9	-4.4	-8.4	-12.5	-16.9
1997 average absolute SHIFOR error	3.8	10.2	16.8	22.1	26.2	28.3
No. of cases	239	239	208	176	148	109
1990-96 average official error (bias)	-1.0	-1.5	-2.3	-3.8	-5.2	-5.8
1990-96 average absolute official error	3.0	7.0	12.0	15.9	18.5	21.4
1990-96 average SHIFOR error (bias)	-1.0	-3.2	-6.1	-9.3	-11.7	-16.0
1990-96 average absolute SHIFOR error	3.0	7.9	13.0	17.1	20.0	23.5
No. of cases	1909	1905	1724	1548	1373	1062

ative at all forecast periods, as is the SHIFOR climatological/persistence statistical wind speed model in 1997 and during the previous 6 yr. A negative bias means that the forecast wind speed is not as high as the best track wind speed. The absolute wind speed errors were somewhat larger than the previous 6-yr averages at all forecast periods, as were the SHIFOR errors.

Acknowledgments. NHC's Lixion Avila, Max Mayfield, Richard Pasch, and Ed Rappaport contributed to the writing of this report and Stephen Baig produced the track charts. Thanks to Chris Velden of the Uni-

versity of Wisconsin Space Science and Engineering Center for providing the satellite imagery.

REFERENCES

Dvorak, V. F., 1984: Tropical cyclone intensity analysis using satellite data. NOAA Tech. Rep. NESDIS 11, 47 pp.
 Trenberth, K. E., 1997: The definition of El Niño. *Bull. Amer. Meteor. Soc.*, **78**, 2771-2777.
 Whitney, L. D., and J. S. Hobgood, 1997: The relationship between sea surface temperatures and maximum intensities of tropical cyclones in the eastern North Pacific Ocean. *J. Climate*, **10**, 2921-2930.